Journal of Solid State Chemistry 183 (2010) 844–848

Contents lists available at ScienceDirect

Journal of Solid State Chemistry

journal homepage: www.elsevier.com/locate/jssc

Order-to-disorder phase transformation in ion irradiated uranium-bearing delta-phase oxides $RE_6U_1O_{12}$ (RE=Y, Gd, Ho, Yb, and Lu)

M. Tang [a,*], K.S. Holliday [b], C. Jiang [a], J.A. Valdez [a], B.P. Uberuaga [a], P.O. Dickerson [a], R.M. Dickerson [a], Y. Wang [a], K.R. Czerwinski [b], K.E. Sickafus [a]

[a] Materials Science and Technology Division, Mail-Stop G755, Los Alamos National Laboratory, Los Alamos, NM 87545, USA
[b] Radiochemistry Group, University of Nevada, Las Vegas, NV 89154, USA

ARTICLE INFO

Article history:
Received 2 November 2009
Accepted 22 January 2010
Available online 1 February 2010

Keywords:
Uranate
Irradiation damage effects
Phase transformation
TEM
XRD

ABSTRACT

Polycrystalline uranium-bearing compounds $Y_6U_1O_{12}$, $Gd_6U_1O_{12}$, $Ho_6U_1O_{12}$, $Yb_6U_1O_{12}$, and $Lu_6U_1O_{12}$ samples were irradiated with various ions species (300 keV Kr^{++}, 400 keV Ne^{++}, and 100 keV He^{+}) at cryogenic temperature (~100 K), and the microstructures were examined following irradiation using grazing incidence X-ray diffraction and transmission electron microscopy. The pristine samples are characterized by an ordered, fluorite derivative structure, known as the delta phase. This structure possesses rhombohedral symmetry. Amorphization was not observed in any of the irradiated samples, even at the highest dose ~65 dpa (displacement per atom). On the other hand, some of these compounds experienced an order-to-disorder (*O–D*) phase transformation, from an ordered rhombohedral to a disordered fluorite structure, at ion doses between 2.5 and 65 dpa, depending on ion irradiation species. Factors influencing the irradiation-induced *O–D* transformation tendencies of these compounds are discussed in terms of density functional theory calculations of the *O–D* transformation energies.

1. Introduction

Uranium (U) and rare earth (*RE*) oxides are important materials for nuclear energy applications. *RE* oxides exhibit considerable solid solubility in nuclear fuel materials made from uranium oxides. *RE*–U–O solid solutions, which crystallize in structures relate to the fluorite (CaF_2) crystal structure [1], are considered as potential fuel forms for transmutation of actinides or waste forms for actinide disposal. The purpose of the study presented here is to examine radiation damage behavior in some specific compounds in the *RE*–U–O system with the formula $RE_6U_1O_{12}$. These compounds can be synthesized using conventional ceramic processing, specifically by heating in air above 1273 K mixtures of uranium oxide and rare earth sesquioxide in a ratio *RE*:U=6:1 [2]. These "6:1:12" compounds are characterized by rhombohedral crystal symmetry and belong to space group $R\overline{3}$. These compounds also possess highly ordered fluorite-related superstructures and are typically referred to in the literature as delta (δ) phase compounds [2,3]. The superstructure of δ-phase, compared to the parent fluorite phase, is due to ordering of both the *RE* and U cations on the cation sublattice, as well as to ordering of the oxygen "vacancies" on the anion sublattice [4]. The U^{6+} cations occupy the 3*a* Wyckoff equipoint in *VI*-fold, distorted octahedral coordination relative to nearest neighbor O anions, while the RE^{3+} cations occupy the general 18*f* equipoint with *VII*-fold coordination relative to surrounding O anions. The formally vacant anion sites, relative to the ideal MO_2 parent fluorite phase, are located at the 6*c* equipoint positions on the triad axes. There are also small relaxations of the U, *RE*, and O ions from their ideal fluorite positions. It is important to note that if U and *RE* cations could randomly swap positions on the cation sublattice sites, and if oxygen ions and oxygen vacancies were to become randomly distributed on all anion sublattice sites, then the cation and anion superlattices associated with delta phase are destroyed and the crystal structure would be indistinguishable (from a diffraction perspective) from the parent fluorite (MO_2) structure. We refer to this crystal structure as the *disordered fluorite* structure. Since radiation damage inherently involves disordering processes, we might anticipate a radiation-induced order-to-disorder (*O–D*) phase transformation, from an ordered rhombohedral to a disordered fluorite phase, in our uranium-bearing delta phase compounds exposed to irradiation. Such a radiation-induced *O–D* transformation has been reported in similar fluorite derivative compounds, such as $A_2B_2O_7$ pyrochlore oxides [5] (where *A* and *B* are metal cations and O are oxygen anions) and $A_4B_3O_{12}$ delta phase oxides [6].

In this paper, we report different *O–D* transformation tendencies of the compounds $Y_6U_1O_{12}$, $Gd_6U_1O_{12}$, $Ho_6U_1O_{12}$, $Yb_6U_1O_{12}$, and $Lu_6U_1O_{12}$ under three different ion irradiation

* Corresponding author. Fax: +1 505 667 8021.
E-mail address: mtang@lanl.gov (M. Tang).

0022-4596/$ - see front matter © 2010 Elsevier Inc. All rights reserved.
doi:10.1016/j.jssc.2010.01.020

conditions: 300 keV Kr^{++}, 400 keV Ne^{++}, and 100 keV He^{+}. We also compare and contrast these experimental results with the *O–D* transformation energies calculated using density functional theory.

2. Experimental procedure

Polycrystalline $Y_6U_1O_{12}$, $Gd_6U_1O_{12}$, $Ho_6U_1O_{12}$, $Yb_6U_1O_{12}$, and $Lu_6U_1O_{12}$ samples were synthesized from Y_2O_3, Gd_2O_3, Ho_2O_3, Yb_2O_3, Lu_2O_3 powders from Alpha Aesar (99.9%–99.99% purity), and UO_2 powder from Bio-Analytical Industries, by conventional ceramic processing procedures [7]. XRD measurements on these samples showed that the sintered pellets consisted of phase-pure $RE_6U_1O_{12}$. Ion irradiations were performed at cryogenic temperature ($\sim$100 K) in the Ion Beam Materials Laboratory at Los Alamos National Laboratory, using a Danfysik high current ion implanter operating at 150 kV. The 300 keV Kr^{++}, 400 keV Ne^{++}, and 100 keV He^{+} ions were implanted at normal incidence using a dose rate of 1×10^{16} ions/m^{2}s to fluences of 2×10^{20} Kr/m^2, 1×10^{20} Ne/m^2, and 1×10^{21} He/m^2. Irradiated samples were analyzed using both grazing incidence X-ray diffraction (GIXRD) and transmission electron microscopy (TEM). GIXRD measurements were performed using a Bruker AXS D8 Advanced X-ray diffractometer at gracing incidence angle of α=0.35°, 1°, and 1°, for Kr, Ne, and He irradiated samples, respectively. Under these conditions, X-rays are scattered from the near-surface of these samples within a depth significantly shallower than the range of these ions (calculated ion ranges are $\sim$200 nm for Kr, $\sim$700 nm for Ne, $\sim$600 nm for He, based on SRIM simulations [7]); X-ray penetration estimates are based on the critical angle formula from Ref. [8]. Thus, we believe that our GIXRD measurements interrogate only the irradiated volume near the sample surface. Irradiated samples were prepared in cross-sectional geometry for TEM examination using a focused-ion-beam (FIB) instrument. TEM investigations were performed using a Philips CM-30 instrument operating at 300 kV.

3. Results and discussion

Fig. 1 shows grazing incidence X-ray diffraction (GIXRD) patterns obtained from U-bearing compounds before and after 300 keV Kr^{++}, 400 keV Ne^{++}, and 100 keV He^{+} ion irradiations. In all of the GIXRD patterns shown in Fig. 1, there are five prominent diffraction peaks labeled "*F*". We will refer to these reflections as parent fluorite peaks (these peaks index as {111}, {200}, {220}, {311}, and {222}, respectively, assuming a structure with a fluorite unit cell). These peaks are the only allowed reflections in the angular range shown (20–70°) for an oxide with the fluorite crystal structure. All other diffraction maxima in the patterns shown in Fig. 1 are fluorite structural derivative or "superlattice" reflections labeled "*R*". These peaks are due to the rhombohedral δ-phase. Specifically, these extra peaks arise from three particular features of the 6:1:12 δ-phase: (1) a small rhombohedral distortion from the ideal cubic symmetry associated with the parent fluorite structure; (2) an ordered arrangement of A^{3+} and U^{6+} cation on the cation sublattices; and (3) an ordered arrangement of vacancies on the oxygen sublattice.

GIXRD results in Fig. 1 can be summarized as follows:

(1) Fig. 1a. Before irradiation, $Gd_6U_1O_{12}$ is initially an ordered δ-phase. Upon ion irradiations almost all *R* peaks associated with the fluorite structural derivative disappear and only *F* peaks remain). This is true for the following irradiation conditions: (1) 2×10^{20} Kr/m^2 (corresponding to 55 dpa); (2) 1×10^{20} Ne/m^2 (corresponding to 3.5 dpa); and (3) 1×10^{21} He/m^2 (corresponding to 2.5 dpa). The irradiated $Gd_6U_1O_{12}$ is transformed to a disordered fluorite under these irradiations. Another important result is that no irradiation-induced amorphization was observed in the irradiated $Gd_6U_1O_{12}$ samples. Similar structural evolution was observed in ion irradiated $Yb_6U_1O_{12}$ (data not shown here).

(2) Fig. 1b. Before irradiation, $Lu_6U_1O_{12}$ is initially an ordered δ-phase. Upon ion irradiations some of the *R* peaks remain, while others exhibit diminished intensity. This is true for the following irradiation conditions: (1) 2×10^{20} Kr/m^2 (corresponding to 65 dpa); (2) 1×10^{20} Ne/m^2 (corresponding to 4 dpa); and (3) 1×10^{21} He/m^2 (corresponding to 2.5 dpa). We interpret these results as indicative of a partial *O–D* phase transformation in $Lu_6U_1O_{12}$. Once again, no amorphization was observed in the irradiated $Lu_6U_1O_{12}$ samples. Similar structural evolution was observed in ion irradiated $Ho_6U_1O_{12}$ and $Y_6U_1O_{12}$ (data not shown here).

Fig. 2 shows cross-sectional TEM bright-field micrographs with corresponding microdiffraction (μD) patterns, obtained from $Gd_6U_1O_{12}$ irradiated under the following conditions: (1) 300 keV

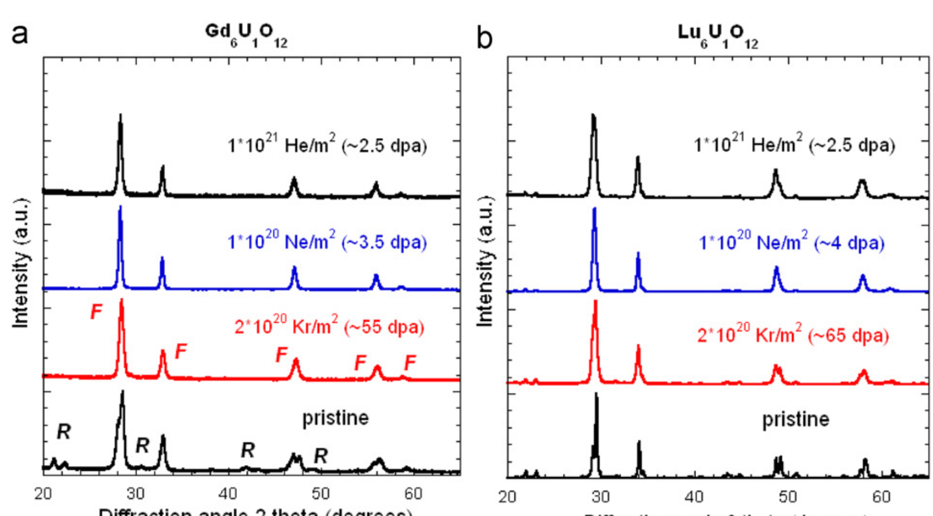

Fig. 1. Grazing incidence X-ray diffraction (GIXRD) patterns obtained from $Gd_6U_1O_{12}$ (a) and $Lu_6U_1O_{12}$ (b) before and after 300 keV Kr^{++}, 400 keV Ne^{++}, and 100 keV He^{+} ion irradiation.

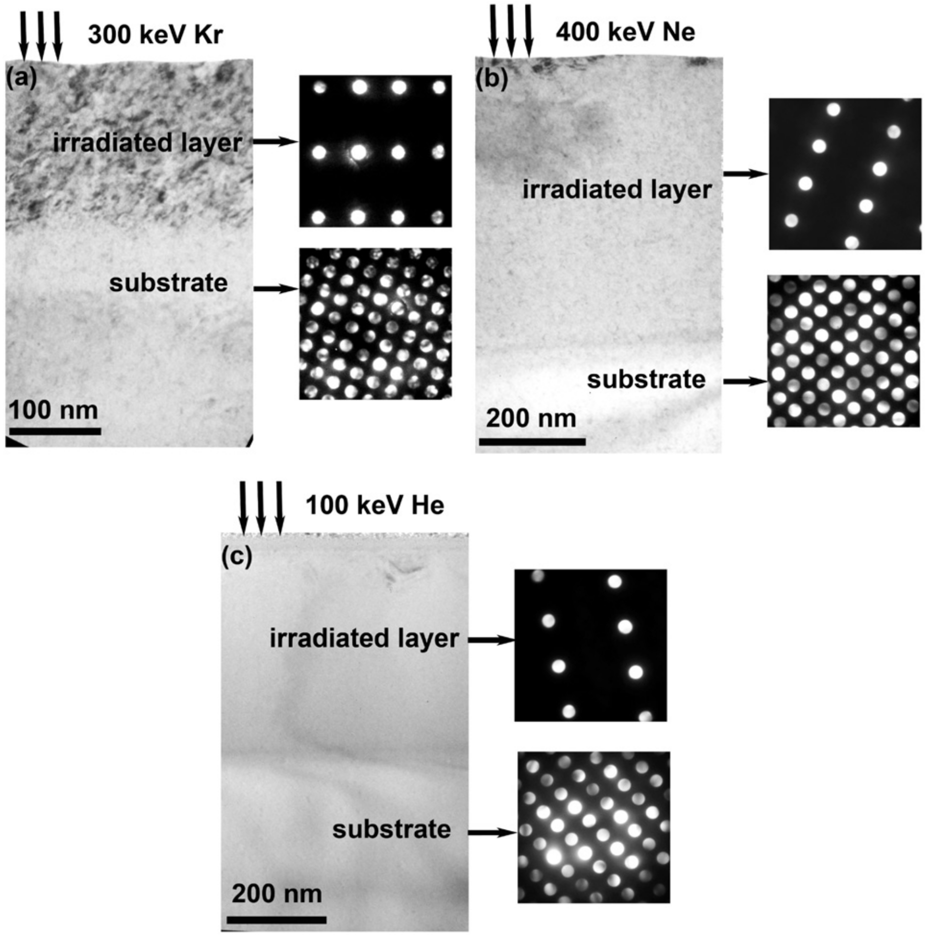

Fig. 2. Cross-sectional TEM bright-field images and corresponding microdiffraction (μD) patterns obtained from $Gd_6U_1O_{12}$ irradiated with (a) 300 keV Kr to a fluence of 2×10^{20} Kr/m^2, (b) 400 keV Ne to a fluence of 1×10^{20} Ne/m^2, and (c) 100 keV He to a fluence of 1×10^{21} He/m^2.

Kr^{++} to a fluence of 2×10^{20} Kr/m^2 (Fig. 2a); (2) 400 keV Ne^{++} to a fluence of 1×10^{20} Ne/m^2 (Fig. 2b); and (3) 100 keV He^{+} to a fluence of 1×10^{21} He/m^2 (Fig. 2c). The μD patterns obtained from the irradiated regions in Figs. 2a,b,c are consistent with a single phase, cubic fluorite structure, oriented with an epitaxial relationship w.r.t the unirradiated substrate. In Figs. 2a, b the beam direction is $\check{B}=[112]_F$ in the irradiated region and $\check{B}=[211]_\delta$ in the substrate (the latter using 3-index, $h\,k\,l$, hexagonal indices). In Fig. 2c, the beam direction is $\check{B}=[013]_\delta$ in the irradiated region and $\check{B}=[1\bar{1}2]_\delta$ in the substrate. TEM observations in Fig. 2 corroborate the GIXRD results presented in Fig. 1a, indicating that $Gd_6U_1O_{12}$ experiences an *O–D* structural transformation induced by Kr/Ne/He ion irradiations, from an ordered δ-phase to a structure indistinguishable from a cubic fluorite. Also, TEM observations revealed no evidence for an irradiation-induced amorphous structure under irradiations. The nature of the *O–D* transformation is described below.

The irradiation-induced *O–D* transformation observed in the δ-phase compounds in this study, can be readily visualized with the aid of a layer-stacking model for the crystal structure of δ-$RE_6U_1O_{12}$. This model is shown in Fig. 3, where we envision the δ-phase as consisting of layers of atoms stacked along the *c*-axis of the hexagonal unit cell. There are 3 metal (*M*) layers and 6 oxygen (O) layers per hexagonal unit cell. The *M* layers can be described as fully-dense, triangular atom nets, while the O layers are based on triangular atom nets, but with ordered arrangements of interstices ("missing" O atoms) [9]. Experimental studies of δ-$RE_6U_1O_{12}$ indicate that the *RE* and U atoms within the *M* layers are fully ordered (see, e.g., Ref. [3] for δ-$Y_6U_1O_{12}$). Essentially, the *M* sublattice in δ-$RE_6U_1O_{12}$ consists of a pseudo-cubic-close-packed arrangement of cations, where 6/7 of the *M* atoms in each *M* layer are *RE* atoms arranged in a $3^4.6$ Archimedean tiling pattern [9]. The remaining 1/7 *M* atoms in each *M* layer are U atoms and these U atoms fill the "holes" in the *RE* $3^4.6$ Archimedean tiling pattern. This defines the super-ordering in δ-$RE_6U_1O_{12}$ compounds due to cation "patterning". In addition, there is also atomic super-ordering in δ-$RE_6U_1O_{12}$ compounds, due to special atomic arrangements on the O sublattice. The anions in the each O layer in a δ-phase compound are arranged in a $3^4.6$ Archimedean tiling pattern, just like the *RE* atoms in the *M* layers [9]. This pattern is shown in Fig. 3. O atom "patterning" produces a super-periodicity of the O sublattice, compared to a cubic fluorite compound. In a cubic MO_2 fluorite-structured oxide, the O layers consist simply of fully-dense, triangular atom nets (same as the *M* layers).

The *O–D* structural transformation in δ-$RE_6U_1O_{12}$ compounds, induced by ion irradiation, apparently is due to rearrangements of atoms on both the *M* and O sublattices. If cation antisite defects are formed under irradiation on the *M* sublattices (*RE* and U atoms exchange positions on the *RE* and U sublattices, respectively), then the $3^4.6$ Archimedean tiling patterns of *RE* atoms in the *M* layers are disturbed. Similarly, if Frenkel pairs form under irradiation on the O sublattice (O atoms and corresponding vacant O sites exchange positions) then the $3^4.6$ Archimedean tiling patterns in the O layers are disturbed. The atomic "patterns" in the *M* and O layers evolve during irradiation, from ordered to random arrangements. Eventually, when the concentration of cation

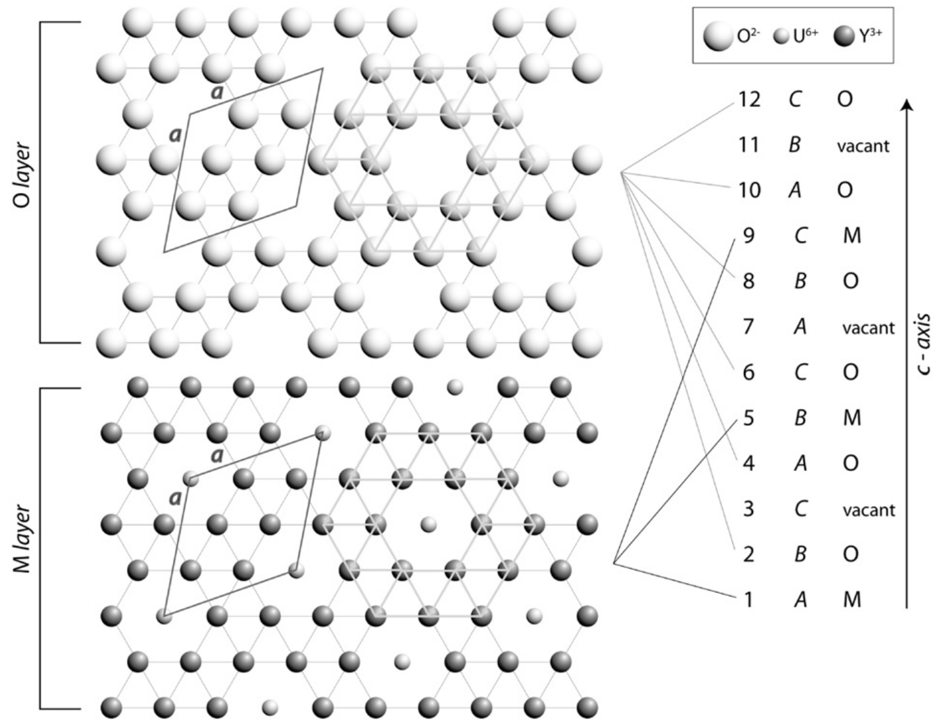

Fig. 3. Schematic diagram showing the stacking and structure of the layers along the *c*-axis for the hexagonal description of δ-phase $RE_6U_1O_{12}$. This drawing uses δ-$Y_6U_1O_{12}$ as an example (spheres representing Y^{3+}, U^{6+} and O^{2-} are shown in the legend, upper right). The $3^4.6$ Archimedian tiling pattern that defines the arrangements of O^{2-} ions in the anion (O) layers and Y^{3+} ions in the cation (*M*) layers, is inscribed on the O and *M* layer drawings. The base of one hexagonal unit cell (edge lengths equal the *a* lattice parameter) is also inscribed on these drawings. There are 12 layers per hexagonal unit cell, labeled 1–12. The translational registry changes between layers to form a face-centered cubic (*fcc*) type of stacking (labeled *ABCABC*…). There are 3 empty layers per hexagonal unit cell (labeled *vacant*).

antisite and anion Frenkel pairs is sufficient, the *M* and O layers, from a diffraction perspective, become indistinguishable from triangular atom nets. By consequence, the irradiated structure comes to resemble a cubic fluorite structure. This is the nature of the *O–D* transformation in δ-$RE_6U_1O_{12}$ compounds, induced by ion irradiation.

To gain some insight into the disordering process under irradiation, we performed first-principles calculations to determine the *O–D* phase transformation energies in these U-bearing δ-phase compounds (results shown in Fig. 4). In order to estimate the *O–D* energetics of $RE_6U_1O_{12}$ (*RE*=Y, Lu, Ho, Gd, and Yb) δ-phases, we have also considered a fully disordered version of the delta phase, i.e., the $(RE_{6/7}U_{1/7})(O_{6/7}V_{1/7})_2$ defect-fluorite structure (where V represents an oxygen vacancy). Here, both the cations and anions are randomly distributed on their respective sublattices. We adopted the special quasirandom structure (SQS) approach [10–12] to adequately reproduce the statistics of such a disordered structure in a relatively small (thus computationally feasible) 76-atom periodic supercell (see Ref. [13] for details on construction of the two-sublattice SQS). First-principles calculations are performed using the all-electron projector augmented wave (PAW) method [14] within the generalized gradient approximation of Perdew, Burke, and Ernzerh of (PBE-GGA) [15], as implemented in Vienna ab initio simulation package (VASP) [16]. According to our convergence tests, a plane wave cutoff energy of 400 eV and a $2\times2\times2$ *k*-point sampling are sufficient to give converged results. By computing the quantum mechanical forces and stress tensor, the lattice parameters and internal atomic positions of all structures are fully optimized using a conjugate-gradient scheme. Finally, the *O–D* disordering energy can be obtained from the total energy difference between the fully ordered ground state delta-phase structure and the SQS, based on which the *O–D* transition

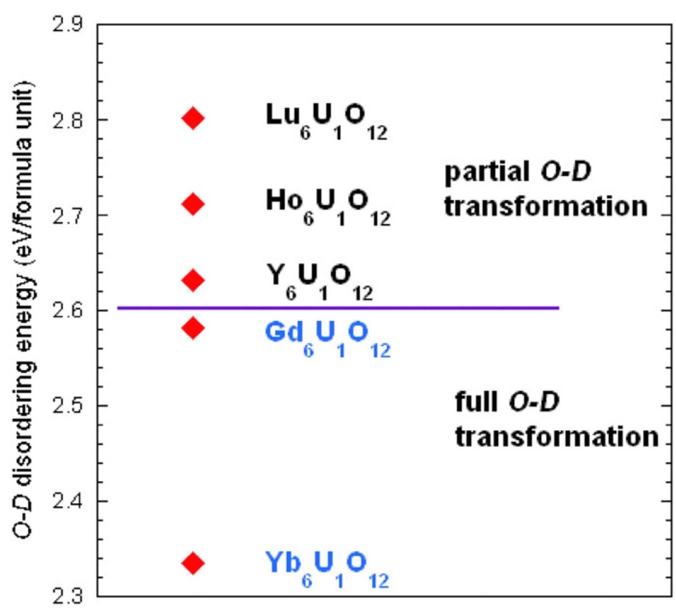

Fig. 4. The order-disorder (*O–D*) transformation energy calculated using density functional theory, for the following uranium-bearing delta phase compounds: $Y_6U_1O_{12}$, $Gd_6U_1O_{12}$, $Ho_6U_1O_{12}$, $Yb_6U_1O_{12}$, and $Lu_6U_1O_{12}$.

temperature can be further estimated [13]. Fig. 4 shows the calculated *O–D* energies for the $RE_6U_1O_{12}$ compounds examined in this study. $Gd_6U_1O_{12}$ and $Yb_6U_1O_{12}$ compounds have lower *O–D* energies compared to other three compounds. This might indicate that the *O–D* phase transformation may occur more readily in these two delta phase compounds. This is, in fact, what was found in the experimental results presented here.

Finally, it is noteworthy that our results may indicate an ion species spectrum effect w.r.t. radiation-induced damage accumulation. Though we did not perform a systematic investigation of spectrum effects in this study, our results seem to indicate that defect survivability (damage efficiency) is enhanced under light ion (He or Ne) compared to heavy ion (Kr) irradiation conditions. Similar enhanced defect survivability under light ion irradiation conditions was recently found in the 4:3:12 δ-phase compounds $Sc_4Zr_3O_{12}$ [17]. This appears to be a somewhat of unusual behavior for ceramic compounds. Work is in progress to further elucidate spectrum effects in U-bearing, $RE_6U_1O_{12}$ δ-phase oxides.

4. Conclusion

We performed 300 keV Kr^{++}, 400 keV Ne^{++}, and 100 keV He^{+} ion irradiation experiments under cryogenic conditions (100 K) on the following polycrystalline δ-phase compounds: $Y_6U_1O_{12}$, $Gd_6U_1O_{12}$, $Ho_6U_1O_{12}$, $Yb_6U_1O_{12}$, and $Lu_6U_1O_{12}$. GIXRD measurements and TEM observations revealed no evidence for irradiation-induced amorphization of these uranium-bearing compounds, up to a maximum dose of 65 dpa. On the other hand, some of these compounds experienced a partial or full order-to-disorder (*O–D*) phase transformation. The disordering tendencies predicted by DFT calculations (particularly, the *O–D* transformation energies), are consistent with the experimental results. This concurrence between theory and experiment may help us to predict the radiation damage tolerance (or damage sensitivity) of specific ceramic compounds. In turn, this will help us to develop new materials as actinide hosts for advanced nuclear fuel or waste forms.

Acknowledgments

This work was sponsored by the Seaborg Institute for Transactinium Science, Los Alamos National Laboratory, and the US Department of Energy, Office of Basic Energy Sciences, Division of Materials Sciences and Engineering.

References

[1] A.J. Freeman, C. Keller, Handbook On the Physics and Chemistry of the Actinides, Elsevier Science Publishers B.V, 1991.
[2] E.A. Aitken, S.F. Bartram, E.F. Juenke, Inorg. Chem. 3 (1964) 949.
[3] S.F. Bartram, Inorg. Chem. 5 (1966) 749.
[4] H.J. Rossell, H.G. Scott, J. Phys. (Paris) Colloq. 38 (1977) C7-28.
[5] R.C. Ewing, W.J. Weber, J. Lian, J. Appl. Phys. 95 (2004) 5949.
[6] K.E. Sickafus, R.W. Grimes, J.A. Valdez, A. Cleave, M. Tang, M. Ishimaru, S.M. Corish, C.R. Stanek, B.P. Uberuaga, Nature Mater. 6 (2007) 217.
[7] J.F. Ziegler, J.P. Biersack, U. Littmark, The Stopping and Range of Ions in Solids, Pergamon Press, New York, 1985.
[8] A. Guinier, X-ray Diffraction in Crystals Imperfect Crystals and Amorphous Bodies, Dover Publications, Inc., New York, 1994.
[9] K.E. Sickafus, R.W. Grimes, S.M. Corish, A.R. Cleave, M. Tang, C.R. Stanek, B.P. Uberuaga, J.A. Valdez, Layered atom arrangements in complex materials, Los Alamos Series Report # LA-14205 (2006).
[10] A. Zunger, S.H. Wei, L.G. Ferreira, J.E. Bernard, Phys. Rev. Lett. 65 (1990) 353.
[11] S.H. Wei, L.G. Ferreira, J.E. Bernard, A. Zunger, Phys. Rev. B 42 (1990) 9622.
[12] C. Jiang, C. Wolverton, J. Sofo, L.Q. Chen, Z.K. Liu, Phys. Rev. B 69 (2004) 214202.
[13] C. Jiang, C.R. Stanek, K.E. Sickafus, B.P. Uberuaga, Phys. Rev. B 79 (2009) 104203.
[14] G. Kresse, J. Joubert, Phys. Rev. B 59 (1999) 1758.
[15] J.P. Perdew, K. Burke, M. Ernzerhof, Phys. Rev. Lett. 77 (1996) 3865.
[16] G. Kresse, J. Furthmuller, Phys. Rev. B 54 (1996) 11169.
[17] J. Zhang, Y.Q. Wang, M. Tang, J. Won, J.A. Valdez, K.E. Sickafus, J. Mater. Res. 25 (2010) 248.